ARTICLE
Journal of Cellular Biochemistry 105:824–834 (2008)

Journal of Cellular Biochemistry

Changes in MicroRNA Expression Patterns in Human Fibroblasts After Low-LET Radiation

Olivier C. Maes,[1] Jin An,[1] Harshini Sarojini,[1] Honglu Wu,[2] and Eugenia Wang[1*]

[1] *Gheens Center on Aging, Department of Biochemistry and Molecular Biology, University of Louisville, Louisville, Kentucky 40292*

[2] *Radiation Biophysics Laboratory, NASA Johnson Space Center, Houston, Texas 77058*

ABSTRACT

Exposure to radiation provokes cellular responses controlled in part by gene expression networks. MicroRNAs (miRNAs) are small non-coding RNAs which mostly regulate gene expression by degrading the messages or inhibiting translation. Here, we investigated changes in miRNA expression patterns after low (0.1 Gy) and high (2.0 Gy) doses of X-ray in human fibroblasts. At early (0.5 h) and late (6 and 24 h) time points, irradiation caused qualitative and quantitative differences in the down-regulation of miRNA levels, including miR-92b, 137, 660, and 656. A transient up-regulation of miRNAs was observed after 2 h post-irradiation following high doses of radiation, including miR-558 and 662. MicroRNA levels were inversely correlated with targets from mRNA and proteomic profiling after 2.0 Gy of radiation. MicroRNAs miR-579, 608, 548-3p, and 585 are noted for targeting genes involved in radioresponsive mechanisms, such as cell cycle checkpoint and apoptosis. We suggest here a model in which miRNAs may act as ''hub'' regulators of specific cellular responses, immediately down-regulated so as to stimulate DNA repair mechanisms, followed by up-regulation involved in suppressing apoptosis for cell survival. Taken together, miRNAs may mediate signaling pathways in sequential fashion in response to radiation, and may serve as biodosimetric markers of radiation exposure. J. Cell. Biochem. 105: 824–834, 2008.

KEY WORDS: FIBROBLAST; LOW LINEAR ENERGY TRANSFER; MICRORNA; RADIATION

MicroRNAs (miRNA) are a large family of small non-coding RNAs of 18–24 nucleotides that generally act as negative post-transcriptional gene regulators [Ruvkun et al., 2004; Nilsen, 2007]. A single miRNA may have broad effects on gene expression networks, such as regulating cell lineage specificity [Liao et al., 2008], cellular functions [Ambros, 2004], or stress response [Marsit et al., 2006]. By partially binding to complementary 3′-untranslated region (UTR) elements of their target mRNAs, miRNAs may repress translation or induce degradation of mRNAs. In fact, levels of miRNA inversely correlate with mRNA levels [Sood et al., 2006], and directly alter mRNA levels [Lim et al., 2005].

Any given miRNA may target up to a thousand different genes, each of which harbors several different miRNA response elements [Maziere and Enright, 2007]. Experimentally, the study of miRNA over-expression and its impact on gene expression profiles has allowed the identification of down-regulated targets and functions for miRNAs [Wang and Wang, 2006]. Alternatively, parallel investigation of miRNA, mRNA and protein expression profiling, and correlation with target predictions, may also reveal genuine microRNA-mediated regulatory networks [Wang and Wang, 2006; Ivanovska et al., 2008]. We have used this approach to identify lead miRNAs implicated in mechanisms of aging and disease [Schipper et al., 2007; Maes et al., 2008].

Disease-related deregulation in miRNA expression has most notably been identified in cancer [Mendell, 2005]. In fact, miRNA expression profiles accurately classify various tumors, and thus provide new diagnostic biomarkers [Lu et al., 2005]. Application of miRNAs to anticancer therapy has also been proposed, such as the use of anti-sense let-7b to promote cell survival in lung epithelial cells after radiation [Weidhaas et al., 2007]. The effect of radiation on miRNA expression appears to vary according to cell type, radiation dose, and post-irradiation time point. For example, 2 h after 7.5 Gy of ^{137}Cs radiation, a decrease in miRNA levels was observed in mouse embryonic fibroblasts, while it increased in embryonic stem cells [Ishii and Saito, 2006]. In contrast, 2.5 Gy of γ-irradiation induced little change in miRNA expression in

Additional supporting information may be found in the online version of this article.

Grant sponsor: National Aeronautics and Space Administration, NASA Johnson Space Center, Houston, Texas; Grant number: NNJ06HF62G.

*Correspondence to: Dr. Eugenia Wang, PhD, Department of Biochemistry and Molecular Biology, University of Louisville School of Medicine, 580 South Preston Street, Louisville, KY 40202. E-mail: eugenia.wang@louisville.edu

Received 3 June 2008; Accepted 11 July 2008 • DOI 10.1002/jcb.21878 • 2008 Wiley-Liss, Inc.

Published online 26 August 2008 in Wiley InterScience (www.interscience.wiley.com)

transformed lymphoblasts after 4 h [Marsit et al., 2006], whereas both down- and up-regulated miRNAs were observed at various post-irradiation time points in lung epithelial cells [Weidhaas et al., 2007]. Interestingly, very high dose X-ray (20.0 Gy) induced long-term up-regulation of miR-194 in a distal body part in rat, a phenomenon known as the bystander effect following radiation exposure [Koturbash et al., 2007]. Bystander response also occurs after low X-ray doses, known to amplify cellular damage and induce apoptosis in neighboring cells [Nelson, 2003; Prise et al., 2003].

Low linear energy transfer (LET) radiation, including ionizing radiation such as X rays, causes cellular damage proportional to the dose and duration of exposure. Acute exposure to low-LET radiation causes DNA damage and apoptosis, while continual exposure eventually triggers cancer [Fujimori et al., 2005]. Although high-LET radiation causes more DNA damage and mutation [Wu et al., 2002; Kawata et al., 2004; Elmore et al., 2006], low-LET radiation at doses as low as 0.02 Gy also causes DNA damage [Leatherbarrow et al., 2006], and induces cellular apoptosis [Portess et al., 2007]. Despite its potential health risk, low-LET radiation may nevertheless trigger an adaptive response in cells to subsequent higher exposures, by preconditioning up-regulation of functions such as DNA repair mechanisms [Pant et al., 2003].

In this study, miRNA expression profiling was investigated in human foreskin fibroblasts following acute exposure to low (0.1 Gy) and high (2.0 Gy) doses of low-LET radiation. We show that radiation induced dose-dependent changes (both qualitative and quantitative) in miRNA levels. The immediate response to radiation exposure was a decrease in miRNA levels, followed by a transient increase after 2 h post-irradiation, especially with the 2.0 Gy exposure. We also provide correlations of miRNA levels with expression levels of their target genes, from direct proteomic and genomic profiling, after 2.0 Gy of radiation. Our results suggest that groups of miRNAs appear to act in concert in response to low-LET radiation, in order to mediate pathways needed to execute cellular stress responses and repair mechanisms.

MATERIALS AND METHODS

CELL CULTURE AND IRRADIATION

Normal human foreskin fibroblasts (AG1522) of low passage [Wu et al., 2002] were routinely cultured at 37°C in 95% humidity and 5% CO_2, in α-MEM medium (Invitrogen, Carlsbad, CA) containing 10% fetal bovine serum (Invitrogen). Confluent cell cultures were irradiated with 250 kV X rays at two dose levels, either 0.1 or 2 Gy, at NASA's Johnson Space Center (JSC, Houston, TX). The exposure at 2 Gy took 3.2 min; that at 0.1 Gy took 42 s. All other chemicals below were obtained from Sigma-Aldrich (St. Louis, MO).

PROTEIN EXTRACTION AND IMMUNOBLOT

Total protein was extracted using RIPA buffer (150 mM NaCl, 10 mM Tris, pH 7.2, 0.01% SDS, 1.0% Triton X-100, 1% Deoxycholate, 5 mM EDTA pH 8.0) containing 1× Protease Inhibitor (Calbiochem, San Diego, CA). Cells were homogenized in 2 volumes (g/ml) of RIPA buffer, and centrifuged at 10,000*g* for 10 min. One volume of RIPA buffer was added to the pellet, sonicated 3 × 10 s, centrifuged, and supernatants were pooled. Protein concentration was determined by the Bradford method (Bio-Rad, Hercules, CA).

Total protein was separated by 9% and 12% SDS–PAGE, and blotted on nitrocellulose membrane Protran BA 85 (Whatman, Schleicher & Schuell, Springfield Mill, Maidstone, Kent, UK) as described [Sarojini et al., 2007]. Primary antibodies tested were anti-human Annexin II (610069, BD Biosciences, San Jose, CA); anti-human Collagenase-1 (MMP-1, clone X2A, Thermo Fischer Scientific, Waltham, MA); anti-human EeF1A [Ruest et al., 2002]; Fibronectin A (P1H11) and Galectin-1 (H-45) from Santa Cruz Biotechnology, Inc. (Santa Cruz, CA). Anti-alpha tubulin (ab7291; Abcam, Cambridge, UK) was used as the loading control. Anti-mouse or rabbit HRP-conjugated secondary antibodies (sc2004, sc2064; Santa Cruz Biotechnology, Inc.) were revealed using SuperSignal West Pico Chemiluminescent Substrate, as per manufacturer's instructions (Pierce Biotechnology, Inc., Rockford, IL). Densitometric quantification of protein levels was performed using ImageQuant 5.2 (Molecular Dynamics, GE HealthCare, Piscataway, NJ), and lanes were normalized using alpha-tubulin levels.

TOTAL AND SMALL RNA EXTRACTIONS

Total RNA extraction and small RNA enrichment were performed as previously described [Schipper et al., 2007; Maes et al., 2008]. Briefly, total RNA was adjusted to 400 μl with RNase-free water, and then 50 μl of NaCl (5 M) and 50 μl of PEG 8000 (v/v 50%) were added. Samples were incubated on ice for 2 h, and centrifuged for 10 min at 13,000 rpm (4°C). Supernatant containing small RNA was transferred to a microcentrifuge tube, and 50 μl of sodium acetate (3 M, pH 4.6) and 1 ml of 100% ethanol were added. The samples were mixed and incubated at −20°C for 2 h, and centrifuged for 10 min at 12,000*g* (4°C). The supernatant was discarded; the pellet was washed with 1 ml of cold 75% ethanol, and then centrifuged for 10 min at 12,000*g* (4°C). The small RNA pellet was dried and dissolved in 12 μl of RNase-free water at 60°C for 10 min. Nucleic acid concentrations were determined at 260 nm by spectrophotometry; samples were stored at −80°C.

MICRORNA PROFILING

Our human microRNA microarray (MMChip) consisted at the time of 462 human anti-sense DNA sequences of mature microRNAs obtained from miRBase (http://microrna.sanger.ac.uk/, version 7.0), spotted and UV crosslinked on nitrocellulose membrane, as described by Wang et al. [2002]. Small RNA samples were labeled with digoxigenin (DIG) at the 3′ end using the DIG Oligonucleotide Tailing Kit, 2nd Generation (Roche Diagnostics, Indianapolis, IN); 1 μg of small RNA was labeled in a total volume of 20 μl. Microarray hybridization and microRNA detection were performed as previously described [Schipper et al., 2007; Maes et al., 2008]. Microarray data were analyzed with SAM software, version 3.02 (Significance Analysis of Microarrays, Stanford University, Stanford, CA). Hierarchical clustering analysis was performed using GenePattern software (www.broad.mit.edu/cancer/software/genepattern/).

QRT-PCR VALIDATION

For real time PCR validation, 0.1 μg of small RNA was quantified using the NCode miRNA First-Strand cDNA Synthesis and qRT-PCR kit (Invitrogen). Mature DNA sense sequences (miRBase, http://microrna.sanger.ac.uk/) of tested miRNAs were used as forward PCR primers. 5S rRNA served as reference gene, and was probed using an internal forward primer (CAGGGTCGGGCCTGGTTAGTACTTG). All real time PCR reactions were performed on a 7500 Fast System Real Time PCR cycler (Applied Biosystems, Foster City, CA), according to manufacturer's instructions. MicroRNA fold changes were calculated by the delta Ct method.

GENE EXPRESSION PROFILING

A broad coverage of the human genome (approximately 6424 unique genes) was analyzed using the National Institute on Aging's Human MGC 17K cDNA microarray (National Cancer Institute's Mammalian Gene Collection; http://mgc.nci.nih.gov/). Total RNA was purified using RNeasy columns (QIAGEN, Inc., Valencia, CA) according to the manufacturer's instructions. Data acquisition and analysis were performed as described [Maes et al., 2007]. Kolmogorov–Smirnov statistics were generated by Gene Set Enrichment Analysis (GSEA) software [Subramanian et al., 2005].

PROTEOMICS

Total protein (150 μg) was precipitated with 6 volumes of cold acetone (−20°C), and then allowed to decant at −20°C. Protein denaturing, reduction and cysteine blocking were done according to manufacturer's instructions (iTRAQ™ labeling kit, Applied Biosystems). Samples were digested by trypsin (Promega, Madison, WI) for 16 h at 37°C. iTRAQ™ reagents 114, 115, 116, and 117 were used to label samples at 0 Gy, 2 Gy/0.5 h, 2 Gy/2 h, and 2 Gy/24 h, respectively. Peptides were fractionated on a 4.6 mm × 20 cm PolySulfoethyl A cation column (PolyLC, Inc., Columbia, MD) using a BioCAD workstation (Applied Biosystems), as previously described [Cong et al., 2006].

Fractions were desalted using the C18 zip tip (Millipore Corporation, Billerica, MA) prior to LC-MS/MS. A QSTAR™ XL hybrid liquid tandem mass spectrometry (LC-MS/MS) system (Applied Biosystems) interfaced with an 1100 Series Capillary LC system (Agilent, Santa Clara, CA) with an analytical 75 μm × 150 mm Vydac MS C18 300A HPLC column (Alltech Associates, Inc., Nicholasville, KY) was used for peptide fractionation and identification. MS-TOF scans were acquired from m/z 350 to 1,600, with up to two precursors selected for MS/MS from 60 to 2,000 m/z, using information-dependent acquisition and rolling collision energy applied to promote fragmentation. Nanospray MS and MS/MS data from the QSTAR™ System were analyzed using Pro QUANT 1.0 software (Applied Biosystems) for both identification and quantification. N-termini, lysine, tyrosine and cysteine modifications were selected as fixed, methionine oxidation as variable, one missed cleavage allowed, precursor error tolerance at <0.15 Da, and product ion error tolerance at <0.1 Da.

FUNCTIONAL ATTRIBUTION

MicroRNA targets were downloaded from the miRBase website (http://microrna.sanger.ac.uk). The Sanger Institute's miRBase is currently one of the most up-to-date resources, with accurate predictions of potential targets using the miRanda algorithm. While other more specific seed match methods of target predictions are available (including PicTar and TargetScan), the loosely conserved and wobble pairing targets known to occur with miRNAs are included in miRBase [Maziere and Enright, 2007]. Therefore our correlations are not restricted to stringent target predictions, and provide a wider range of potential targets. Proteomic and gene expression data were inversely correlated with target predictions for each miRNA. Functional attribution to genes and proteins was made according to the SOURCE database (http://source.stanford.edu). Functional attribution to miRNAs was based on functional enrichment of the correlated predicted targets at $P < 0.01$, using the Gene Ontology Tree Machine (GOTM; http://bioinfo.vanderbilt.edu/gotm).

RESULTS

MICRORNA EXPRESSION PROFILING

MicroRNA expression was assessed at 0.5, 2, 6, and 24 h post-irradiation in foreskin fibroblasts, after low (0.1 Gy) and high (2.0 Gy) doses of low-LET radiation in triplicate for each time point. Only highly significant microRNA expressions are reported, using stringent 0–6% false discovery rates. The general effect of radiation on miRNA expression was a decrease in several miRNAs at 0.5, 6, and 24 h post-irradiation time, with an interrupted increase in miRNA levels after 2 h. The changes were most significant after high-dose irradiation (2.0 Gy), as determined by T-statistics (Fig. 1 and Table I). A similar expression pattern occurred after 0.1 Gy of irradiation for the same miRNAs, but their levels were not

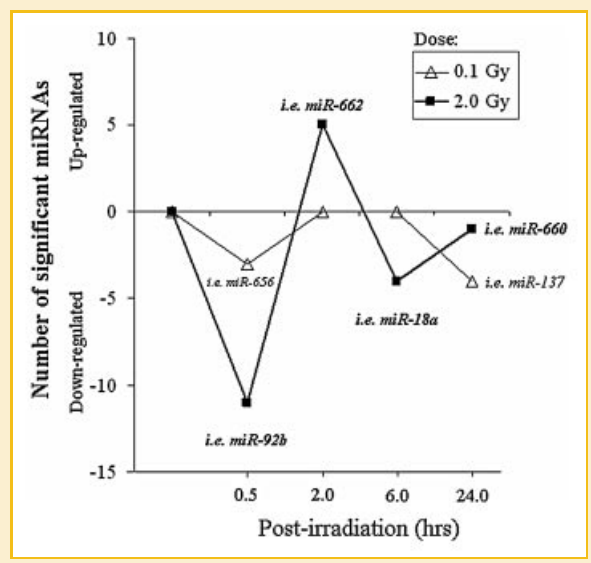

Fig. 1. Number of significantly up- and down-regulated microRNAs after low-LET irradiation. MicroRNA (miRNA) expression profiling was assessed after 0.5, 2, 6, and 24 h post-irradiation time following 0.1 or 2.0 Gy of X-rays, in foreskin fibroblasts. Examples of miRNAs are indicated at specific post-irradiation time points. A full list of the significant miRNAs, with T-statistics, is reported in Table I.

TABLE I. MicroRNA Expression After Low-LET Radiation

Radiation dose 0.1 Gy				Radiation dose 2.0 Gy			
Gene name	Fold	Score (d)	q-value (%)	Gene name	Fold	Score (d)	q-value (%)
Post-irradiation time: 0.5 h							
hsa-miR-656	0.5	−2.5	0.0	hsa-miR-92b	0.5	−3.0	0.0
hsa-miR-421	0.4	−2.2	0.0	hsa-miR-617	0.6	−2.2	0.0
hsa-miR-648	0.5	−1.6	0.0	hsa-miR-517c	0.6	−2.1	0.0
				hsa-miR-609	0.6	−2.0	0.0
				hsa-miR-564	0.5	−1.9	0.0
				hsa-miR-520d*	0.3	−1.9	0.0
				hsa-miR-663	0.6	−1.9	0.0
				hsa-miR-608	0.4	−1.9	0.0
				hsa-miR-623	0.6	−1.8	0.0
				hsa-miR-223	0.6	−1.8	0.0
				hsa-miR-579	0.6	−1.8	0.0
				hsa-miR-192	0.6	−1.8	0.0
Post-irradiation time: 2 h							
				hsa-miR-662	2.6	2.3	0.0
				hsa-miR-558	2.6	2.0	0.0
				hsa-miR-582-5p	1.7	1.9	0.0
				hsa-miR-548b-3p	1.9	1.8	0.0
				hsa-miR-585	1.6	1.7	0.0
Post-irradiation time: 6 h							
				hsa-miR-18a	0.6	−3.0	0.0
				hsa-miR-609	0.6	−2.8	0.0
				hsa-miR-188-5p	0.7	−2.7	0.0
				hsa-miR-181b	0.5	−2.2	0.0
Post-irradiation time: 24 h							
hsa-miR-137	0.7	−3.1	0.0	hsa-miR-660	0.8	−1.8	0.0
hsa-miR-376a*	0.7	−1.9	0.0				
hsa-miR-659	0.6	−1.7	0.0				
hsa-miR-598	0.8	−1.7	0.0				

False discovery rate correspond to the q-value (%).

significantly different from control non-irradiated cultures. Although low-dose (0.1 Gy) radiation had a lower quantitative affect on miRNA expression, significant qualitative differences were nevertheless observed at 0.5 and 24 h post-irradiation (Table I). For example, at 0.5 h post-irradiation, an initial decrease in the level of miR-656 was observed after low dose, whereas miR-92b significantly decreased after high dose. At 24 h post-irradiation, however, low-dose radiation had a greater impact on the number of miRNAs with significant decreases in expression (Table I).

We next determined the miRNA expression patterns as a function of radiation dosage (0.1 and 2.0 Gy) and time post-irradiation (0.5, 2, 6, 24 h). Only miR-137 showed a significant time course-dependent response, with a gradual decrease from 2 to 24 h after both 0.1 and 2.0 Gy doses of irradiation (Fig. 2). In contrast, several miRNAs showed significant expression patterns by principal component analysis (eigengene quantitative response) between non-irradiated controls, 0.1 and 2.0 Gy irradiated cell cultures (Fig. 2 and Supplementary Table SI). Interestingly, most miRNAs followed the expression pattern illustrated in Figure 1, that is, down-regulated at 0.5, 6, and 24 h, with an interrupted transient up-regulation at 2 h.

The expression patterns described above were validated by real time qPCR for a down-regulated (miR-92b) and an up-regulated (miR-662) miRNA, as well as for two miRNAs (miR-18a, 376a*) with significant expression patterns (Fig. 3). As with the microarray platform, we obtained greater quantitative changes after 2.0 Gy of irradiation. For example, the expression pattern of miR-18a (i.e., decrease at 0.5 h, increase at 2 h, and decrease again at 6 h), mainly detected after 2.0 Gy of radiation, was confirmed by qPCR. The decrease in miR-376a* was also validated in both low- and high-dose irradiated fibroblasts after 6 and 24 h. Although not highly significant on the microarray platform, an increase in miR-376a* at 2 h after 2 Gy of irradiation was estimated by qPCR. The decrease in miR-92b at 0.5 h was equally validated by qPCR after both doses of radiation. Likewise, the increase in miR-662 at 2 h was validated after 2.0 Gy of radiation.

Next, miRNA expression patterns were analyzed by hierarchical clustering (Fig. 4). To compare expression profiles between experimental factors (time and radiation dose), the average ratio of the hybridization intensity over control values was used to normalize each experimental condition. As expected, the magnitudes of down-regulation at 0.5, 6, and 24 h, and up-regulation of miRNAs at 2 h (as indicated by the colored scale), were more pronounced after high (2.0 Gy) than low (0.1 Gy) doses of X rays. Importantly, the expression profiles at each post-irradiation time point cluster separately, with doses of radiation grouped at their respective time points.

GENE EXPRESSION PROFILING

Gene expression profiles of fibroblasts exposed to 2.0 Gy of X-rays were analyzed at 2 and 24 h post-irradiation in triplicate for each time point (Table II and Supplementary Table SII). A significant up-regulation of genes was observed at 2 h, whereas a significant down-regulation was mostly observed at 24 h (Supplementary Fig. S1). Kolmogorov–Smirnov statistics (Gene set enrichment analysis, GSEA) revealed several genes similarly up- or down-regulated after 2 and 24 h post-treatment (Supplementary Fig. S2).

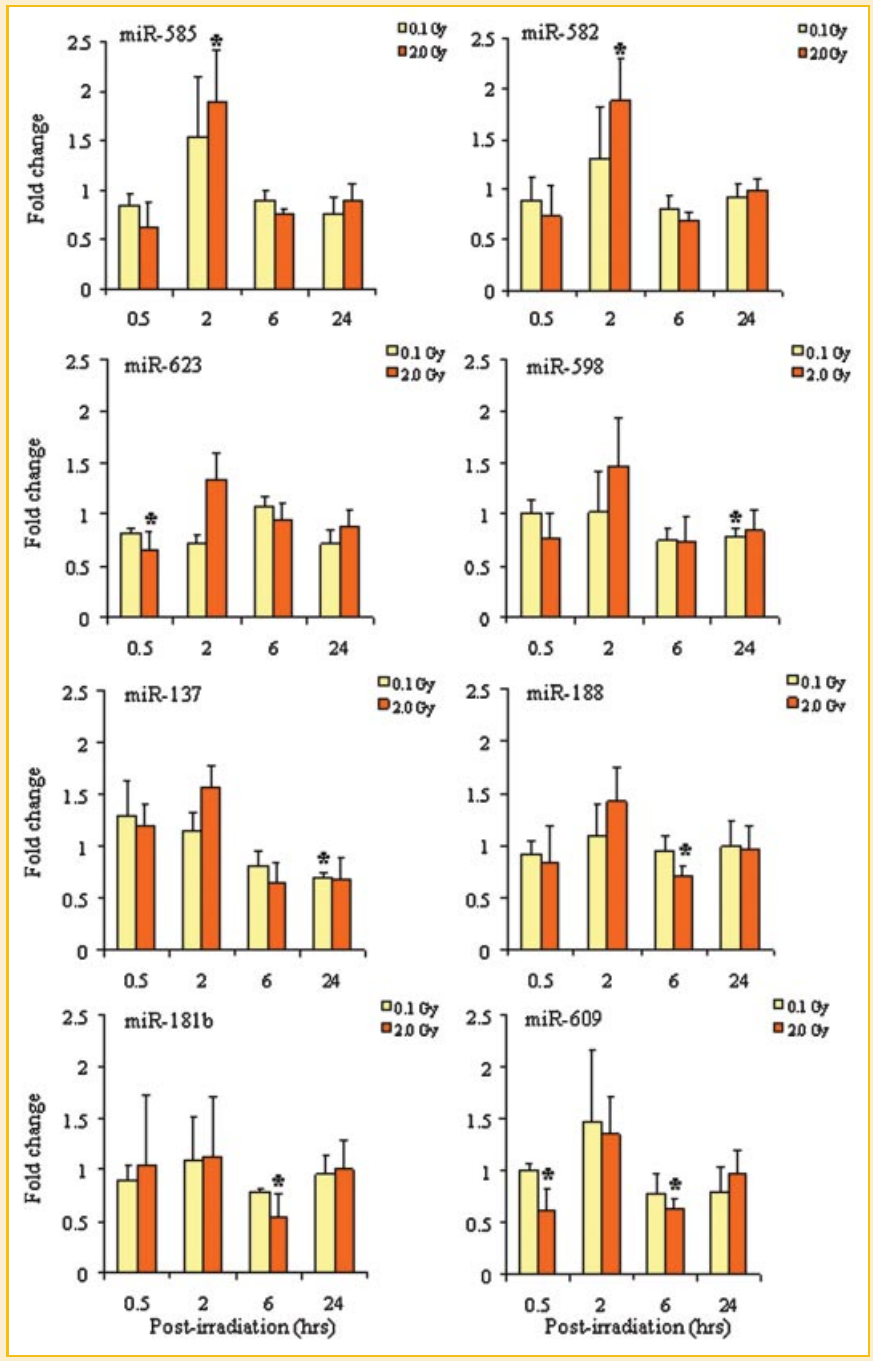

Fig. 2. Principal component analysis of microRNA expression patterns. Expression patterns of miRNAs were analyzed in non-irradiated controls and irradiated cultures (0.1 and 2.0 Gy) at each post-irradiation time point. Fold changes in miRNA levels compared to non-irradiated controls were calculated from average hybridization intensity values. Bars represent standard error. Statistics are reported in Supplementary Table SI. [Color figure can be viewed in the online issue, which is available at www.interscience.wiley.com.]

At 2 h post-irradiation, three major up-regulated genes were metallothionein 2A (MT2A), matrix metalloproteinase 1 (MMP-1), and cyclin-dependent kinase inhibitor 1A (CDKN1A). Genes with a continual increase in expression at both 2 and 24 h include CDKN1A, cystatin C (CST3), and ribosomal protein S24 (RPS24). Several genes were found to decrease at both 2 and 24 h, including collagen type II (COL2A1), cold shock domain protein A (CDA), and filamin A (FLNA). The increase in MMP-1 mRNA levels at 2 h (Supplementary Table SII) was validated at the protein level, with 1.2- and 1.4-fold increases at 2 and 24 h respectively (Supplementary Fig. S3).

The enriched Gene Ontology (GO) biological categories for the up-regulated genes at 2 h were apoptosis, cellular homeostasis and negative regulation of proliferation. The down-regulated GO

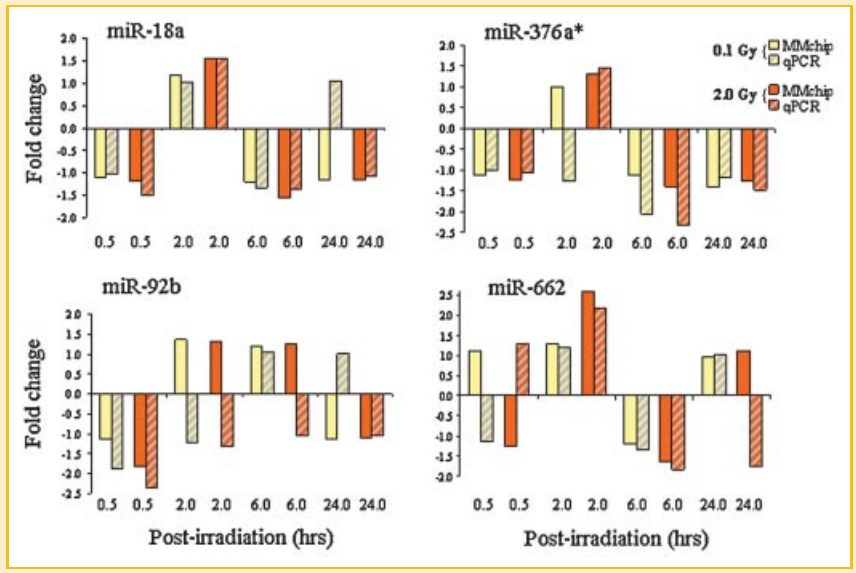

Fig. 3. Validation of microRNA array platform (MMchip) by qPCR. Fold changes in miRNA levels after 0.1 and 2.0 Gy of X-rays compared to non-irradiated controls are reported for each post-irradiation time point. Fold changes were estimated at each time points in triplicate by the delta Ct method. [Color figure can be viewed in the online issue, which is available at www.interscience.wiley.com.]

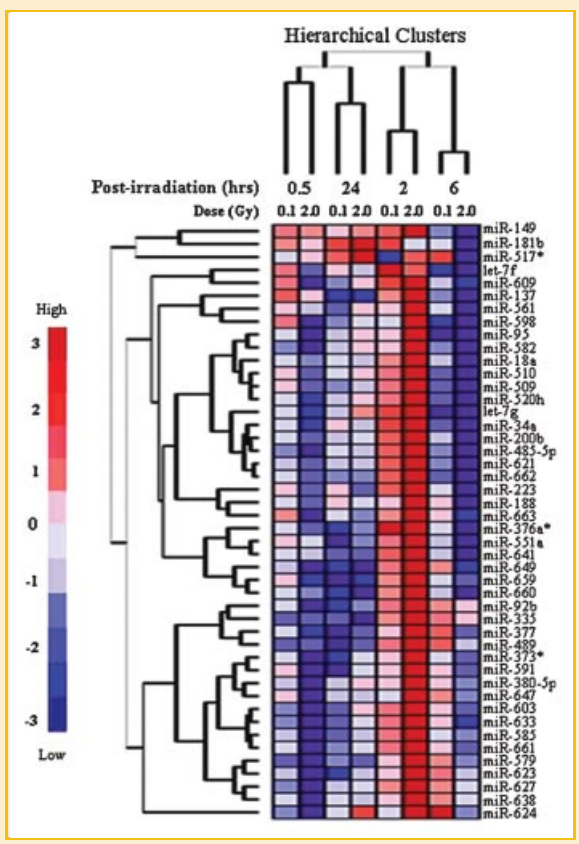

Fig. 4. Hierarchical cluster analysis of microRNA expression after low-LET radiation. Hierarchical clusters were generated using Pearson correlations of miRNA expression patterns after 0.5, 2, 6, and 24 h following 0.1 and 2.0 Gy of X-ray exposure. The up- (red) and down-regulated (blue) miRNAs were scaled according to the depicted color code. [Color figure can be viewed in the online issue, which is available at www.interscience.wiley.com.]

biological categories were cell adhesion, protein kinase cascade, and protein biosynthesis. After 24 h, down-regulated GO categories were cell cycle checkpoint, cytoskeleton biogenesis, and DNA repair.

PROTEOMIC PROFILING

Proteomics of fibroblasts exposed to 2 Gy of X-rays were analyzed at 0.5, 2, and 24 h post-irradiation time points (Table III and Supplementary Table SIII). Known biodosimeter proteins were detected at a confidence cutoff set at >95%. For example, calreticulin (CALR [Ramsamooj et al., 1995]) and filamin A (FLNA [Meng et al., 2004]) were found to increase at both 0.5 and 24 h post-irradiation. Interestingly, some proteins were found to initially increase at 0.5 h, decrease at 2 h, and then increase again at 24 h, such as elongation factor 1-alpha 1 (EEF1A1). Proteins that specifically increased at 2 h include annexin II (ANXA2) and galectin 1 (LGALS1). iTRAQ quantifications were validated by immunoblotting for annexin A2, EEF1A1, and galectin-1 (Supplementary Fig. S4). Importantly, the fluctuating levels of EEF1A1 and galectin-1 were confirmed, validating their down and up trends respectively at 2 h post-irradiation.

The enriched GO biological categories for the proteins detected to increase at all post-irradiation time points (Table II) were cell motility and cytoskeleton processes. The biological GO category protein folding was down-regulated at all time points. At 2 h post-irradiation, the GO category apoptosis is enriched among the up-regulated proteins. GO categories of proteins detected to decrease at 0.5 and 24 h were glycolysis and apoptosis.

FUNCTIONAL ATTRIBUTION OF RADIORESPONSIVE MICRORNA

Predicted miRNA targets [Griffiths-Jones et al., 2006] were compared with the above genomic (Table II) and proteomic data (Table III), using only miRNAs with significantly altered expression after high-dose radiation (2.0 Gy). Since the miRNA action may have

TABLE II. MicroRNA Target Correlation With Gene Expression After 2.0 Gy of Radiation

MicroRNA down at 0.5 h	Target gene	Symbol	Fold	Score (d)	q-value (%)
A					
Up-regulated at 2 h					
miR-92b, 617	Vesicle amine transport protein 1	VAT1	1.5	2.2	0.4
miR-92b	Maternal embryonic leucine zipper kinase	MELK	2.2	1.9	0.8
miR-617, 517c	Proteasome activator subunit 1	PSME1	4.0	3.5	0.0
miR-617	Adenylyl cyclase-associated protein	CAP1	2.0	2.3	0.4
miR-617	Stanniocalcin 2	STC2	4.7	2.1	0.4
miR-617	Vascular endothelial growth factor B	VEGFB	3.2	1.9	0.8
miR-517c	Mitogen-activated protein kinase 7	MAPK7	2.8	1.9	0.8
miR-609	Male-enhanced antigen	MEA1	1.9	1.8	0.8
miR-609	Ribonuclease/angiogenin inhibitor	RNH1	2.0	2.0	0.4
miR-564	Voltage-dependent anion channel 1	VDAC1	3.1	1.9	0.8
miR-564	Cysteinyl-tRNA synthetase	CARS	2.6	1.8	0.8
miR-564	Cytochrome *c* oxidase assembly protein	COX10	1.6	3.0	0.4
miR-564	Copine I	CPNE1	Inf	1.6	1.2
miR-564	Guanine nucleotide binding protein, AI2	GNAI2	6.1	2.1	0.4
miR-564	General transcription factor IIA, 2	GTF2A2	2.0	2.0	0.4
miR-663, 192	Inhibitor of growth family, member5	ING5	4.2	2.2	0.4
miR-663	Mucolipin 1	MCOLN1	2.1	2.0	0.4
miR-608, 564	Flotillin 1	FLOT1	3.8	2.7	0.4
miR-608, 663	Cystatin C	CST3	Inf	2.5	0.4
miR-608, 663	Ribosomal protein S24	RPS24	1.7	1.6	1.2
miR-608	Calreticulin	CALR	1.6	3.3	0.4
miR-608	Cyclin-dependent kinase inhibitor 1A	CDKN1A	4.0	3.9	0.0
miR-608	Ras and Rab interactor 1	RIN1	1.7	1.7	1.2
miR-623	Plakophilin 3	PKP3	5.7	1.9	0.8
miR-623	Splicing factor 1	SF1	3.9	2.0	0.8
miR-223	Dolichyl-phosphate mannosyltransferase 2	DPM2	6.2	1.7	1.1
miR-223	Transmembrane 4 superfamily member 1	TM4SF1	4.3	3.3	0.4
miR-223	Mitochondrial ribosomal protein S7	MRPS7	1.9	2.1	0.4
miR-579, 192	Cathepsin K	CTSK	9.2	1.8	1.1
miR-579	Synovial sarcoma, X breakpoint 2	SSX2	2.3	2.5	0.4
miR-579	Placenta-specific 8	PLAC8	2.6	3.4	0.4
miR-579	Prohibitin	PHB	1.7	3.4	0.4
miR-579	Proteasome subunit, beta type, 7	PSMB7	4.0	1.8	0.8
miR-579	Peroxisomal membrane protein 3	PXMP3	8.6	1.8	0.8
miR-579	Thyroid hormone receptor interactor6	TRIP6	9.6	2.8	0.4
miR-192, 517c	WD repeat domain 8	WDR8	2.7	2.8	0.4
miR-192	Ferritin, heavy polypeptide 1	FTH1	2.3	2.8	0.4
miR-192	Cyclin-dependent kinase 7	CDK7	3.9	2.1	0.4
miR-192	RAB7, member RAS oncogene	RAB7A	2.0	2.3	0.4

MicroRNA up at 2 h	Target gene	Symbol	Fold	Score (d)	q-value (%)
B					
Down-regulated at 2 h					
miR-662, 558	Nucleolar protein family A, member 2	NOLA2	0.2	−2.0	1.2
miR-662	Degenerative spermatocyte homolog, lipid desaturase	DEGS	0.1	−2.1	1.2
miR-662	Ribosomal protein L13	RPL13	0.6	−3.5	1.1
miR-558	Splicing factor 3b, subunit 4, 49 kDa	SF3B4	0.3	−2.7	1.1
miR-558	Transforming growth factor, beta-induced	TGFBI	0.4	−2.2	1.2
miR-582-5p	Actin, alpha 2, smooth muscle, aorta	ACTA2	0.4	−5.4	0.0
miR-582-5p	Serine/threonine kinase 3	STK3	0.0	−2.6	1.1
miR-582-5p, 548b-3p	MAD2 mitotic arrest deficient-like 1	MAD2L1	0.0	−3.0	1.1
miR-582-5p, 548b-3p	Spermidine/spermine N1-acetyltransferase	SAT1	0.1	−2.7	1.1
miR-548b-3p	Ribosomal protein L27	RPL27	0.6	−2.2	1.1
miR-548b-3p	SPARC related modular calcium binding 1	SMOC1	0.0	−3.0	1.1
miR-585	Isoleucine-tRNA synthetase	IARS	0.6	−3.1	1.1
Down-regulated at 24 h					
miR-662, 558, 548b-3p	Dolichyl-phosphate N-acetylglucosaminephosphotransferase 1	DPAGT1	0.3	−1.1	8.0
miR-662, 558	Eukaryotic translation elongation factor 1α1	EEF1A1	0.6	−1.8	4.3
miR-662, 558	Nucleolar protein family A, member 2	NOLA2	0.3	−1.5	4.3
miR-662, 585	Phosphoglucomutase 1	PGM1	0.2	−1.2	7.6
miR-662, 585	Chromosome 21 open reading frame 33	C21orf33	0.6	−1.1	7.6
miR-662	Ribosomal protein L13	RPL13	0.9	−0.9	8.0
miR-662	Tumor suppressing subtransferable candidate 4	TSSC4	0.4	−0.9	8.0
miR-558, 582-5p, 548b-3p	High-mobility group box 2	HMGB2	0.0	−0.8	9.7
miR-558, 582-5p	Histone deacetylase 6	HDAC6	0.6	−1.0	8.0
miR-558	Enolase 1	ENO1	0.6	−1.0	8.0
miR-582-5p	Actin, alpha 2, smooth muscle, aorta	ACTA2	0.5	−3.3	0.0
miR-582-5p	Junctophilin 3	JPH3	0.1	−1.4	4.3
miR-582-5p	Sialophorin (CD43)	SPN	0.4	−3.2	0.0
miR-582-5p, 548b-3p	MAD2 mitotic arrest deficient-like 1	MAD2L1	0.1	−2.1	4.3
miR-548b-3p	SPARC related modular calcium binding 1	SMOC1	0.1	−2.3	4.3
miR-548b-3p	t-complex 1	TCP1	0.6	−0.8	8.0
miR-548b-3p	LIM and SH3 protein 1	LASP1	0.5	−0.9	8.0
miR-548b-3p	Matrilin 2	MATN2	0.1	−1.0	8.0
miR-548b-3p	SH3-domain kinase binding protein 1	SH3KBP1	0.0	−1.3	7.6
miR-585	Calpain 10	CAPN10	0.1	−1.1	7.6
miR-585	Epoxide hydrolase 2, cytoplasmic	EPHX2	0.5	−1.1	8.0
miR-585	Neuromedin B	NMB	0.1	−1.5	4.3
miR-585	Valosin-containing protein	VCP	0.6	−1.1	8.0

T-statistics (d scores) and false discovery rate (q-values) refer to target genes.

TABLE III. MicroRNA Target Correlation With Protein Levels After 2.0 Gy of Radiation

MicroRNA	Protein target	Gene symbol	Accession	Ratio 2 Gy/0 Gy
A				
Down at 30 min	Increase at 30 min			
miR-517c	Desmoyokin	AHNAK	gi|39932548	1.13
miR-663, 608, 617, 564, 579	Filamin-A	FLNA	gi|113001	1.36
miR-663	Alpha-actinin-1	ACTN1	gi|13123942	1.18
miR-608	Calreticulin	CALR	gi|117505	1.38
Down at 30 min	Increase at 2 h			
miR-564	Annexin A2	ANXA2	gi|113950	1.35
miR-579	Fibronectin	FN1	gi|2506872	1.33
miR-579	Proactivator polypeptide	PSAP	gi|134218	1.56
Down at 6 and 24 h	Increase at 24 h			
miR-660	Calreticulin	CALR	gi|117505	1.54
miR-188-5p	Elongation factor 1-alpha 1	EEF1A	gi|3122072	1.19
miR-188-5p	Filamin-A	FLNA	gi|113001	1.45
miR-181b	Desmoyokin	AHNAK	gi|39932548	1.17
B				
Up at 2 h	Decrease at 2 h			
miR-662, -558	Elongation factor 1-alpha 1	EEF1A1	gi|3122072	0.75
miR-585	Actin, cytoplasmic 2	ACTG1	gi|54040660	0.98
miR-548b-3p	Desmoyokin	AHNAK	gi|39932548	0.83
miR-582-5p	Tropomyosin alpha-4 chain	TPM4	gi|54039746	0.99
Up at 2 h	Decrease at 24 h			
miR-662	Heat shock protein 90 kDa beta 1	HSP90B1	gi|6015101	0.70
miR-662	Pyruvate kinase isozyme M1	PKM2	gi|75061500	0.59
miR-558	Peptidyl-prolyl cis-trans isomerase A	PPIA	gi|75061782	0.57
miR-548b-3p	Desmoyokin	AHNAK	gi|39932549	0.54
miR-548b-3p	Histone H2B type 1-C/E/F/G/I	HIST1H2BC	gi|109940083	0.46
miR-548b-3p	Profilin-1	PFN1	gi|51702769	0.54
miR-548b-3p	Vimentin	VIM	gi|55977767	0.77

long-term effects on gene or protein levels, corresponding up- and down-regulated targets were associated with their inversely regulated miRNAs at the same and subsequent time points. For simplification and target correlation purposes, target proteins (Table III) are referred to using their gene symbols.

Down-regulated miRNAs at 0.5 h were correlated with up-regulated targets at 0.5 and 2 h post-irradiation, including miR-579, 564, 608, 192, and 617. These five miRNAs together corresponded to over 65% of the correlations found with the genomic and proteomic data, with miR-579 (17%), 564 (14%), and 608 (14%) exhibiting the most frequent correlations. Up-regulated miRNAs at 2 h correlated with down-regulated targets at 2, 6, and 24 h, including miR-548-3p, 662, 558, and 528-5p. The most frequent correlations of up-regulated miRNAs with target genes and proteins were with miR-548b-3p (27%), followed by miR-662 (22%).

For example, decreased miR-608 levels correlated with increases in CALR protein levels at 0.5 h, as well as CDKN1A mRNA at 2 h post-irradiation. Several down-regulated miRNAs (miR-663, -608, -617, -579, -564) were associated with the increase in FLNA protein levels at 0.5 h. Up-regulated miR-662 at 2 h correlated with a decrease in EEF1A1 protein levels at 2 h, as well as with a decrease in its transcript after 24 h.

Taken together, correlations of predicted targets were mostly observed with the down-regulated miRNAs at 0.5 h, and up-regulated miRNAs at 2 h. The enriched GO biological categories of correlated target genes and proteins at these two time points are summarized in Figure 5. Following 2.0 Gy of X-ray, the immediate decrease in miRNA levels at 0.5 h correlated with an increase in targets involved in functions related to cell cycle check point and DNA repair. Two hours later, up-regulated miRNAs correlated with a decrease in targets involved in functions related to cell cycle check point and apoptosis.

DISCUSSION

In this study, two acute doses of X rays exerted both qualitative and quantitative differences on miRNA expression in human fibroblasts. The immediate response was a two-fold down-regulation of three to four miRNAs following 0.1 Gy (miR-421, 648, 656) and 2.0 Gy (miR-92b, 564, 520d* and 608) of radiation. Interestingly, at the high dose of radiation, a significant impact on the transient up-regulation of miRNAs after 2 h (including miR-662 and 558) was observed, followed by subsequent down-regulation at 6 h post-exposure (including miR-18a and 181b). By 24 h post-irradiation, both low and high doses of radiation induced the down-regulation trend, with more miRNAs responsive to the lower (0.1 Gy) than the higher dose (2.0 Gy). This dose-dependent expression of miRNAs suggests that specific miRNAs may eventually serve as bio-dosimetric markers, to differentiate low from high doses of radiation exposure.

As described above, a time-dependent expression pattern was observed for groups of miRNAs: a down-regulation at 0.5, 6, and 24 h post-irradiation time points, interrupted by an up-regulation at 2 h. A similar up-regulation of several miRNAs after 2 h of radiation (7.5 Gy) has been reported in embryonic stem cells, including miR-181a, 188, and 376a [Ishii and Saito, 2006]. Likewise, we also noted a slight increase in closely related miRNAs at 2 h after radiation exposure. Importantly, we report expression patterns comparable to those reported for several miRNAs after 2, 8, and 24 h following 2.5 Gy of radiation in lung epithelial cells, including miR-92b, 582, 663 [Weidhaas et al., 2007].

Here, miRNAs were inversely correlated with their target levels in order to identify their functional roles in radioresponsive mechanisms. Targets were identified by direct mRNA expression and global tandem mass proteomic profiling after 2 Gy of radiation. Our

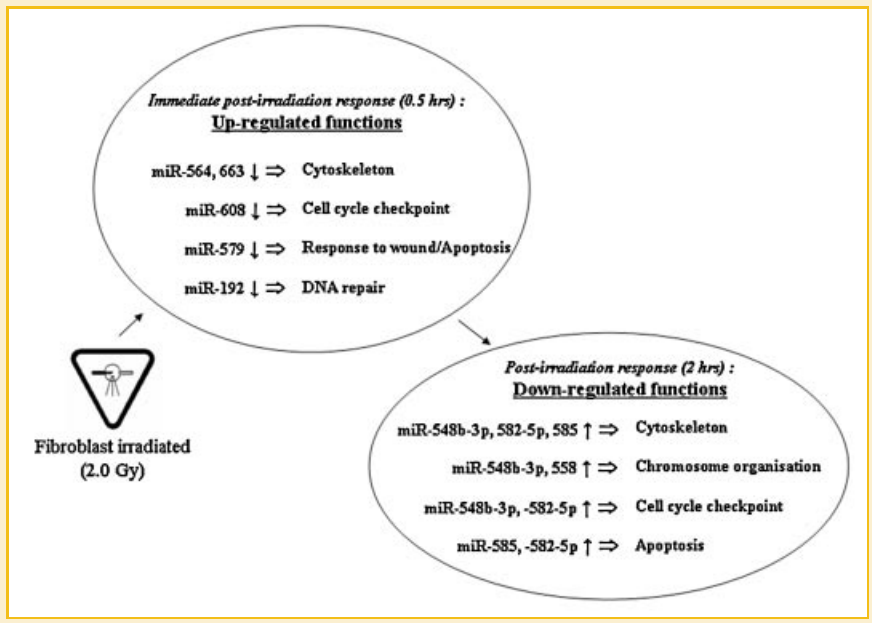

Fig. 5. Model for microRNA-associated radioresponsive mechanisms after low-LET radiation. In this model, miRNAs may act as "hub" regulators of specific cellular responses, immediately down-regulated to stimulate DNA repair mechanisms, followed by up-regulation to suppress apoptosis for cell survival. Levels of target genes and proteins were inversely correlated with miRNA levels (Tables II and III). Functional attributions were based on Gene Ontology category enrichments (GOTM) with P values <0.01.

gene expression results were similar to previous studies, and corresponded to previously reported Gene Ontology categories [Ding et al., 2005]. Known radioresponsive biomarkers were detected in both our genomic and proteomic data, such as cyclin-dependent kinase inhibitor 1A (CDKN1A), fibronectin 1 (FN1), calreticulin (CALR), matrix metalloproteinase 1 (MMP1), and vimentin (VIM) [Heinloth et al., 2003; Ding et al., 2005; Kis et al., 2006; Marchetti et al., 2006; Ao et al., 2008]. Interestingly, similar gene expression patterns of up-regulation at 2 h and down-regulation at 24 h were also described in fibroblasts after ^{137}Cs exposure [Zhou et al., 2006].

We propose a model for cellular radioresponsive mechanisms that may implicate miRNAs in the regulation of the cell cycle checkpoint and apoptotic pathways (Fig. 5). The initial decreases in miR-608, 579 and 192 correlated with the up-regulation of target genes (Table II) and proteins (Table III) involved in cell cycle checkpoint, response to wounding, and DNA repair, respectively. Our results support the notion that radiation-induced DNA damage triggers arrest in proliferation by the cell cycle checkpoint [Zhou et al., 2006]. Moreover, the up-regulation of CDKN1A/p21 is believed to be central to this p53-dependent regulation of the G_1 checkpoint, in order to allow DNA repair following radiation exposure [Kis et al., 2006; Zhou et al., 2006]. MicroRNA-mediated regulation of CDKN1A levels has also been reported for miR-106b in cancer [Ivanovska et al., 2008]. Here, the correlation of miR-608 with CDKN1A corresponded to a high predicted Watson-Crick base pairing score in the 3′UTR region of mRNA (miRBase); and suggests that different miRNAs regulate similar targets in different biological contexts.

Other miR-608 targets are associated with anti-apoptotic (i.e., elongation factor 1A, EEF1A) [Ruest et al., 2002] and cell survival (i.e., calrecticulin, CALR) [Okunaga et al., 2006] functions. Together, this suggests that miR-608 may contribute to cell cycle arrest, in the interest of DNA repair and cell survival. Moreover, the possible miRNA-mediated up-regulation of filamin A (FLNA) is also noteworthy, since it is involved in DNA damage recovery mechanisms [Meng et al., 2004]. In fact, several down-regulated miRNAs (including miR-608 and 579) correlate with the increase in filamin A protein levels.

Two hours after high dose radiation, the up-regulation of miR-548b-3p and 582-5p correlated with the decrease in target genes with cell cycle checkpoint functions (i.e., MAD2 mitotic arrest deficient-like 1, MAD2L1) [To-Ho et al., 2008]. The increase in miR-582-5p and 585 levels also correlated with the repression of targets involved in apoptosis (i.e., valosin-containing protein, VCP) [Zucchini et al., 2008], chromosomal organization (i.e., histone deacetylase 6, HDAC6) [Kwon et al., 2007], as well as cytoskeletal functions (i.e., vimentin, VIM) [Bartel-Friedrich et al., 2007]. Thus, the up-regulation of miR-592-5p, 548b-3p, and 585 may reveal underlying signaling to control the cell cycle checkpoint and apoptosis, so that cell recovery mechanisms may take place.

In summary, our results suggest that multiple miRNAs act in concert to regulate specific responses in post-irradiated foreskin fibroblasts. The initial down-regulation of miRNAs may de-repress the cell cycle check point, and favor DNA repair mechanisms. Other miRNAs up-regulated at 2 h may then be involved to some extent in repressing apoptotic responses in order to rescue the cells from death signaling. Future functional bioassays will be necessary to investigate the function of lead miRNAs identified in our study in controlling cellular radioresponsive pathways. Our study provides evidence that radiation dose is associated with levels of miRNA

abundance; the sensitivity of this response using a wider range of radiation warrants further investigation. It will also be necessary to determine whether miRNA expression is directly altered by radiation, or as a result of downstream cell signaling, including long-term effects. At present, our study suggests that lead microRNAs may become biodosimetric markers, and may prove useful for radioprotective therapy prior to higher LET radiation exposure.

ACKNOWLEDGMENTS

The authors gratefully acknowledge the participation of Megumi Hada, Suying Xu, Leszek Wojakiewicz and Jiawei Zhao. The authors also thank Alan N. Bloch for proofreading this paper.

REFERENCES

Ambros V. 2004. The functions of animal microRNAs. Nature 431:350–355.

Ao X, Lubman DM, Davis MA, Xing X, Kong FM, Lawrence TS, Zhang M. 2008. Comparative proteomic analysis of radiation-induced changes in mouse lung: Fibrosis-sensitive and -resistant strains. Radiat Res 169:417–425.

Bartel-Friedrich S, Lautenschlager C, Holzhausen HJ, Friedrich RE. 2007. Expression and distribution of cytokeratins and vimentin in rat larynx and trachea following irradiation. Anticancer Res 27:2059–2069.

Cong YS, Fan E, Wang E. 2006. Simultaneous proteomic profiling of four different growth states of human fibroblasts, using amine-reactive isobaric tagging reagents and tandem mass spectrometry. Mech Ageing Dev 127:332–343.

Ding LH, Shingyoji M, Chen F, Hwang JJ, Burma S, Lee C, Cheng JF, Chen DJ. 2005. Gene expression profiles of normal human fibroblasts after exposure to ionizing radiation: A comparative study of low and high doses. Radiat Res 164:17–26.

Elmore E, Lao XY, Kapadia R, Redpath JL. 2006. The effect of dose rate on radiation-induced neoplastic transformation in vitro by low doses of low-LET radiation. Radiat Res 166:832–838.

Fujimori A, Okayasu R, Ishihara H, Yoshida S, Eguchi-Kasai K, Nojima K, Ebisawa S, Takahashi S. 2005. Extremely low dose ionizing radiation up-regulates CXC chemokines in normal human fibroblasts. Cancer Res 65:10159–10163.

Griffiths-Jones S, Grocock RJ, van Dongen S, Bateman A, Enright AJ. 2006. miRBase: microRNA sequences, targets and gene nomenclature. Nucleic Acids Res 34:D140–D144.

Heinloth AN, Shackelford RE, Innes CL, Bennett L, Li L, Amin RP, Sieber SO, Flores KG, Bushel PR, Paules RS. 2003. Identification of distinct and common gene expression changes after oxidative stress and gamma and ultraviolet radiation. Mol Carcinog 37:65–82.

Ishii H, Saito T. 2006. Radiation-induced response of micro RNA expression in murine embryonic stem cells. Med Chem 2:555–563.

Ivanovska I, Ball AS, Diaz RL, Magnus JF, Kibukawa M, Schelter JM, Kobayashi SV, Lim L, Burchard J, Jackson AL, Linsley PS, Cleary MA. 2008. MicroRNAs in the miR-106b family regulate p21/CDKN1A and promote cell cycle progression. Mol Cell Biol 28:2167–2174.

Kawata T, Ito H, Uno T, Saito M, Yamamoto S, Furusawa Y, Durante M, George K, Wu H, Cucinotta FA. 2004. G2 chromatid damage and repair kinetics in normal human fibroblast cells exposed to low- or high-LET radiation. Cytogenet Genome Res 104:211–215.

Kis E, Szatmari T, Keszei M, Farkas R, Esik O, Lumniczky K, Falus A, Safrany G. 2006. Microarray analysis of radiation response genes in primary human fibroblasts. Int J Radiat Oncol Biol Phys 66:1506–1514.

Koturbash I, Boyko A, Rodriguez-Juarez R, McDonald RJ, Tryndyak VP, Kovalchuk I, Pogribny IP, Kovalchuk O. 2007. Role of epigenetic effectors in maintenance of the long-term persistent bystander effect in spleen in vivo. Carcinogenesis 28:1831–1838.

Kwon S, Zhang Y, Matthias P. 2007. The deacetylase HDAC6 is a novel critical component of stress granules involved in the stress response. Genes Dev 21:3381–3394.

Leatherbarrow EL, Harper JV, Cucinotta FA, O'Neill P. 2006. Induction and quantification of gamma-H2AX foci following low and high LET-irradiation. Int J Radiat Biol 82:111–118.

Liao R, Sun J, Zhang L, Lou G, Chen M, Zhou D, Chen Z, Zhang S. 2008. MicroRNAs play a role in the development of human hematopoietic stem cells. J Cell Biochem 104:805–817.

Lim LP, Lau NC, Garrett-Engele P, Grimson A, Schelter JM, Castle J, Bartel DP, Linsley PS, Johnson JM. 2005. Microarray analysis shows that some microRNAs down-regulate large numbers of target mRNAs. Nature 433:769–773.

Lu J, Getz G, Miska EA, Alvarez-Saavedra E, Lamb J, Peck D, Sweet-Cordero A, Ebert BL, Mak RH, Ferrando AA, Downing JR, Jacks T, Horvitz HR, Golub TR. 2005. MicroRNA expression profiles classify human cancers. Nature 435:834–838.

Maes OC, Xu S, Yu B, Chertkow HM, Wang E, Schipper HM. 2007. Transcriptional profiling of Alzheimer blood mononuclear cells by microarray. Neurobiol Aging 28:1795–1809.

Maes OC, An J, Sarojini H, Wang E. 2008. Murine microRNAs implicated in liver functions and aging process. Mech Ageing Dev 129:534–541.

Marchetti F, Coleman MA, Jones IM, Wyrobek AJ. 2006. Candidate protein biodosimeters of human exposure to ionizing radiation. Int J Radiat Biol 82:605–639.

Marsit CJ, Eddy K, Kelsey KT. 2006. MicroRNA responses to cellular stress. Cancer Res 66:10843–10848.

Maziere P, Enright AJ. 2007. Prediction of microRNA targets. Drug Discov Today 12:452–458.

Mendell JT. 2005. MicroRNAs: Critical regulators of development, cellular physiology and malignancy. Cell Cycle 4:1179–1184.

Meng X, Yuan Y, Maestas A, Shen Z. 2004. Recovery from DNA damage-induced G2 arrest requires actin-binding protein filamin-A/actin-binding protein 280. J Biol Chem 279:6098–6105.

Nelson GA. 2003. Fundamental space radiobiology. Gravit Space Biol Bull 16:29–36.

Nilsen TW. 2007. Mechanisms of microRNA-mediated gene regulation in animal cells. Trends Genet 23:243–249.

Okunaga T, Urata Y, Goto S, Matsuo T, Mizota S, Tsutsumi K, Nagata I, Kondo T, Ihara Y. 2006. Calreticulin, a molecular chaperone in the endoplasmic reticulum, modulates radiosensitivity of human glioblastoma U251MG cells. Cancer Res 66:8662–8671.

Pant MC, Liao XY, Lu Q, Molloi S, Elmore E, Redpath JL. 2003. Mechanisms of suppression of neoplastic transformation in vitro by low doses of low LET radiation. Carcinogenesis 24:1961–1965.

Portess DI, Bauer G, Hill MA, O'Neill P. 2007. Low-dose irradiation of nontransformed cells stimulates the selective removal of precancerous cells via intercellular induction of apoptosis. Cancer Res 67:1246–1253.

Prise KM, Folkard M, Michael BD. 2003. Bystander responses induced by low LET radiation. Oncogene 22:7043–7049.

Ramsamooj P, Notario V, Dritschilo A. 1995. Enhanced expression of calreticulin in the nucleus of radioresistant squamous carcinoma cells in response to ionizing radiation. Cancer Res 55:3016–3021.

Ruest LB, Marcotte R, Wang E. 2002. Peptide elongation factor eEF1A-2/S1 expression in cultured differentiated myotubes and its protective effect against caspase-3-mediated apoptosis. J Biol Chem 277:5418–5425.

Ruvkun G, Wightman B, Ha I. 2004. The 20 years it took to recognize the importance of tiny RNAs. Cell 116:S93–S96, 2 p following S96.

Sarojini H, Medepalli K, Terry DA, Alphenaar BW, Wang E. 2007. Localized delivery of DNA to the cells by viral collagen-loaded silica colloidal crystals. BioTechniques 43:213–221.

Schipper HM, Maes OC, Chertkow HM, Wang E. 2007. MicroRNA expression in Alzheimer blood mononuclear cells. Gene Regulation Syst Biol 1:263–274.

Sood P, Krek A, Zavolan M, Macino G, Rajewsky N. 2006. Cell-type-specific signatures of microRNAs on target mRNA expression. Proc Natl Acad Sci USA 103:2746–2751.

Subramanian A, Tamayo P, Mootha VK, Mukherjee S, Ebert BL, Gillette MA, Paulovich A, Pomeroy SL, Golub TR, Lander ES, Mesirov JP. 2005. Gene set enrichment analysis: A knowledge-based approach for interpreting genome-wide expression profiles. Proc Natl Acad Sci USA 102:15545–15550.

To-Ho KW, Cheung HW, Ling MT, Wong YC, Wang X. 2008. MAD2DeltaC induces aneuploidy and promotes anchorage-independent growth in human prostate epithelial cells. Oncogene 27:347–357.

Wang X, Wang X. 2006. Systematic identification of microRNA functions by combining target prediction and expression profiling. Nucleic Acids Res 34:1646–1652.

Wang E, Lacelle C, Xu S, Zhao X, Hou M. 2002. Designer microarrays: From soup to nuts. J Gerontol A Biol Sci Med Sci 57:B400–B405.

Weidhaas JB, Babar I, Nallur SM, Trang P, Roush S, Boehm M, Gillespie E, Slack FJ. 2007. MicroRNAs as potential agents to alter resistance to cytotoxic anticancer therapy. Cancer Res 67:11111–11116.

Wu H, Furusawa Y, George K, Kawata T, Cucinotta FA. 2002. Analysis of unrejoined chromosomal breakage in human fibroblast cells exposed to low- and high-LET radiation. J Radiat Res (Tokyo) 43(Suppl):S181–S185.

Zhou T, Chou JW, Simpson DA, Zhou Y, Mullen TE, Medeiros M, Bushel PR, Paules RS, Yang X, Hurban P, Lobenhofer EK, Kaufmann WK. 2006. Profiles of global gene expression in ionizing-radiation-damaged human diploid fibroblasts reveal synchronization behind the G1 checkpoint in a G0-like state of quiescence. Environ Health Perspect 114:553–559.

Zucchini C, Rocchi A, Manara MC, De Sanctis P, Capanni C, Bianchini M, Carinci P, Scotlandi K, Valvassori L. 2008. Apoptotic genes as potential markers of metastatic phenotype in human osteosarcoma cell lines. Int J Oncol 32:17–31.